JOURNAL OF SPACECRAFT AND ROCKETS
Vol. 33, No. 4, July–August 1996

Recent Aerothermodynamic Flight Measurements During Shuttle Orbiter Re-Entry

John J. Bertin*
U.S. Air Force Academy, Colorado 80840-6222
Stanley A. Bouslog† and Kuo-Chi Wang‡
Lockheed Martin Engineering and Sciences, Houston, Texas 77258-8561
and
Charles H. Campbell§
NASA Johnson Space Center, Houston, Texas 77058

All four Space Shuttle Orbiters, which are currently operational, have limited instrumentation packages that provide information about the aerothermodynamic environment. Heat transfer rates have been determined from the measured temperature histories using a simple technique. The experimental rates thus determined have been compared with previous flight data and with existing computations. The comparisons were used to evaluate the data in general, to study viscous–inviscid interactions such as those due to body-flap deflections, and to evaluate possible flight anomalies.

Nomenclature

b = span, 23.79 m (78.06 ft)
L = reference length of Shuttle Orbiter, 32.8 m (107.53 ft)
q = local heat transfer rate, W/cm^2; Eq. (1)
q_{ref} = stagnation-point heat transfer rate, W/cm^2; Eq. (3)
R_N = nose radius, m
T_w = wall temperature, K
U_∞ = freestream velocity, m/s
U_{co} = circular orbit velocity, 7950 m/s
X = axial coordinate for the Shuttle Orbiter; Fig. 1
Y = transverse coordinate for the Shuttle Orbiter; Fig. 1
Z = vertical coordinate for the Shuttle Orbiter; Fig. 5
α = angle of attack, deg
δ_{BF} = body-flap deflection angle, deg
ε = surface emissivity
ρ_∞ = freestream density, kg/m^3
ρ_{sl} = sea-level density, kg/m^3
σ = Stefan–Boltzmann constant, 5.67×10^{-8} W/(m^2 K^4)

Introduction

THE conventional approach to flight demonstration through incremental expansion of the flight envelope is not feasible with the Shuttle vehicle. Once the Shuttle is committed to flight, it must complete all mission elements, including launch, ascent, orbit insertion, deorbit, entry, and landing. Thus, during the preflight design phase, NASA and Rockwell International gave careful attention to the development of an aerothermodynamic database derived largely from wind-tunnel tests, with detailed attention being given to defining uncertainties through statistical analysis of wind-tunnel data and by comparisons of wind-tunnel predictions with flight data from previous programs. The development schedule paid particular attention to providing flight data as early as possible to verify that the design procedures utilized reasonable models of the actual environment experienced by the Shuttle. In 1978, Bornemann and Surber[1] noted: "The first six orbital flights of the Shuttle are developmental test flights, and the seventh flight in 1980 is considered the initial operational capability flight." However, in fact, the use of the Space Shuttle Orbiter as a flight research vehicle was limited to the first five flights, designated STS-1 through STS-5 (for Space Transportation System).

As discussed by Throckmorton,[2]

> During the Orbital Flight Test missions (STS-1 through -5), the Orbiter Columbia was equipped with a large complement of diagnostic instrumentation that was referred to as the Development Flight Instrumentation (DFI). DFI measurements were intended to provide the requisite data for postflight certification of Orbiter subsystems designs before the start of Orbital operational missions. The DFI system was composed of over 4500 sensors, associated data-handling electronics, and data recorder:
>
> Included among the DFI and of particular interest to aerothermodynamic researchers were measurements of the Orbiter's aerodynamic surface temperature at over 200 surface locations. These measurements were obtained from thermocouples mounted within the TPS materials, in thermal contact with the TPS surface coatings. The DFI also included temperature measurements in depth, within the TPS materials, at some 19 locations, and along TPS tile sidewalls within the gaps between tiles at 16 locations. Aerodynamic surface pressure measurements were also made in numbers and distribution similar to the surface-temperature measurements.

The data obtained during the flights of STS-1 through STS-5 have been used extensively by researchers to calibrate and to evaluate techniques used to predict the aerothermodynamic environment of a hypersonic vehicle. For example, the temperature histories provided by the thermocouples in thermal contact with the thermal protection system (TPS) surface coatings provided information about boundary-layer transition and were used to assess the accuracy of the Orbiter boundary-layer transition prediction methodology, an example of which is presented in Ref. 3. In addition, special experiments were conducted during these first five flights, including one experiment in which a catalytic overcoat of black iron cobalt spinel in a polyvinyl acetate binder was sprayed onto selected tiles.[4] Surface temperature histories were obtained for baseline tiles and for tiles having an overcoat of high catalytic efficiency. By comparing the temperatures from two such tiles, located side by side, one can get an immediate and positive indication of the relative catalytic efficiency. However, one must compare the data with computed heat transfer rates to obtain a quantitative measure of the catalytic efficiency. Such comparisons have been made by Scott[5] and Rakich

Received March 14, 1995; revision received April 26, 1995; accepted for publication Feb. 9, 1996. Copyright © 1996 by the American Institute of Aeronautics and Astronautics, Inc. No copyright is asserted in the United States under Title 17, U.S. Code. The U.S. Government has a royalty-free license to exercise all rights under the copyright claimed herein for Governmental purposes. All other rights are reserved by the copyright owner.

*Professor, Department of Aeronautics. Fellow AIAA.
†Principal Engineer, P.O. Box 58561. Associate Fellow AIAA.
‡Engineer, P.O. Box 58561.
§Aerospace Engineer, EG3. Member AIAA.

et al.[6] For more than a decade, the results of such investigations of the Shuttle aerothermodynamic environment have appeared in the literature, including the proceedings of NASA conferences, e.g., Refs. 7 and 8.

Data relevant to the aerothermodynamic environment during the re-entry of the Orbiter have been obtained for flights STS-26 to the present. Although the number of sensors on the current fleet of Orbiters is relatively small, the data have nevertheless provided important information about anomalous behavior encountered during specific flights. Surface thermocouples indicated that transition began at 900 s into the re-entry of STS-28. Thermocouples on the Orbiter structure also indicated an increased temperature, which verified that the vehicle had experienced a higher heat load due to turbulent heating. The premature onset of boundary-layer transition during the re-entry of STS-28 was attributed to protruding gap fillers. During the re-entry of STS-50, Orbiter elevon deflections and yaw reaction control jet firings indicated that the vehicle experienced a yawing moment at the same time transition occurred. Surface thermocouple data confirmed that boundary-layer transition occurred on the right side of the vehicle 80 s prior to its occurrence on the left side.

To identify problems such as those described in the previous paragraph in a timely and efficient fashion, it is important to be able to reduce the flight data using simple engineering procedures. Using the approximation that the incident convective heating is proportional to the heat radiated from the surface, the convective heat transfer histories can be easily extracted from the surface temperature histories. This approximation will be used to reduce the data from recent flights. These data will then be compared with data from the re-entry of STS-2 and with computations of the heat transfer generated using existing flowfield computations.[9] A primary objective of this paper is to demonstrate that this simple procedure can be used to produce data that provide reliable information about the aerothermodynamic environment of the Orbiter during a particular re-entry, soon after the vehicle has landed.

Experimentally Determined Heat Transfer Rates

Each of the four currently operational Orbiters has thermocouples mounted within the TPS, in thermal contact with the surface coating. As shown in Fig. 1, there are 11 thermocouples on the Columbia (OV-102), 6 thermocouples on the Discovery (OV-103), 6 thermocouples on the Atlantis (OV-104), and 14 thermocouples on the Endeavour (OV-105). These thermocouples are part of the Modular Auxiliary Data System (MADS), which is similar to the DFI system. Although the Orbiter flown for the STS-2 mission was the Columbia (OV-102), the STS-2 aerothermodynamic instrumentation was the more complete DFI package. Thus, the data from the STS-2 flight will be considered as a special case (rather than included with the post-DFI flights of the OV-102) when discussing the flight-test data.

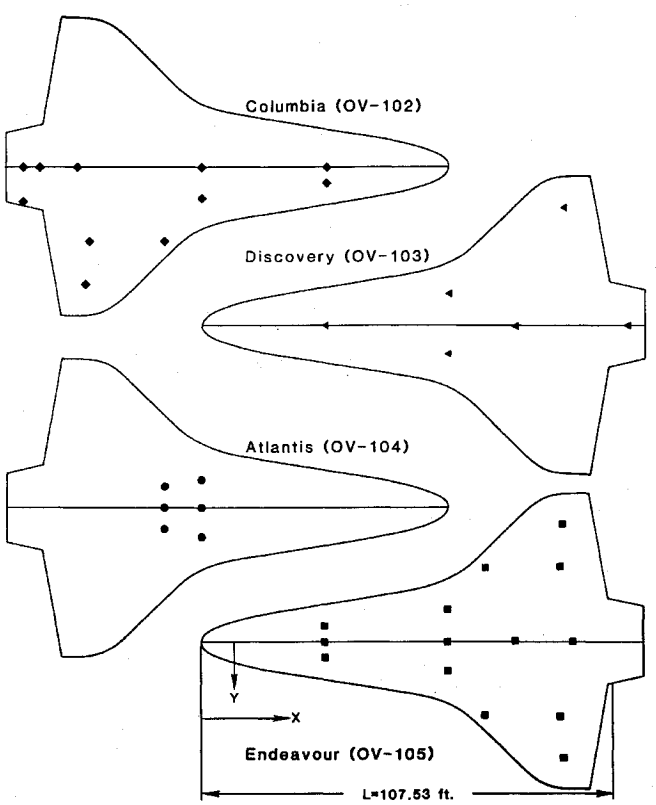

Fig. 1 Thermocouple locations on the current Orbiter fleet.

The temperature histories sensed by the thermocouples on the current Orbiter fleet continue to provide information about the aerothermodynamic environment of the windward surface. Because the thermal conductivity of the Shuttle TPS tiles is low, the heat-flux histories can be determined directly from the temperature histories provided by the thermocouples. The experimentally determined local heat transfer rates presented in this paper for the STS-2 flight as well as for the post-DFI flights were calculated using the measured wall temperatures in the expression

$$q = 1.06\varepsilon\sigma T_w^4 \tag{1}$$

The factor 1.06 was obtained using an inverse thermal math model[10] to take into account conduction into the tile, storage of heat in the surface layer, and the fact that the thermocouple was not precisely on the external surface. In reality, this factor could vary by approximately ±10% over the trajectory to reflect variations in the rate at which heat is conducted and stored within the tile.

The heating rates calculated using Eq. (1) are very sensitive to uncertainties in the surface emissivity. The heat transfer rates presented in this paper assumed that the emissivity is a linear function of temperature:

$$\varepsilon = 0.844 - 0.0000447T_w \tag{2}$$

which is based on data presented by Bouslog and Cunnington.[11] Edwards et al.[12] used a radiometric technique (in which the energy radiated by the subject specimen is compared with the energy radiated by a standard reference at the same temperature and wavelength) to determine the spectral normal emittance of a Space Shuttle reusable surface insulation material. The surface emissivities determined by Edwards et al.[12] show a strong dependence on temperature, decreasing from approximately 0.86 at room temperature to approximately 0.71 at 1300 K. Other investigators use a value $\varepsilon = 0.9$, which is based on emittance measurements made at room temperature and on calculations at elevated temperatures, as described by Throckmorton.[13]

There are other factors that can introduce errors in the experimental heat transfer rates derived from a given temperature history. Uncertainties due to temperature measurements, to the material properties, and to the actual thermocouple locations introduce uncertainties in the experimental values of the heating rate of approximately 7–8%.

The heating rates determined using Eq. (1) were divided by the theoretical heat transfer rate to the stagnation point of a 0.3048-m (1.0-ft) sphere using the equation of Detra et al.[14]:

$$q_{\text{ref}} = \frac{11{,}030}{R_N^{0.5}}\left(\frac{\rho_\infty}{\rho_{\text{sl}}}\right)^{0.5}\left(\frac{U_\infty}{U_{\text{co}}}\right)^{3.15} \tag{3}$$

where the heat transfer rate is in W/cm^2. Values of ρ_∞ and U_∞ for a specific time are taken from the Orbiter project best estimated trajectory for that flight.

The temperature history and the nondimensionalized heat-transfer-rate history for the thermocouple at $X = 0.296L$ in the plane of symmetry for the STS-54 flight of the Endeavour is presented in Fig. 2. The angle of attack is approximately 40 ± 2 deg from 500 to 1100 s. For times from 500 to 900 s, the temperature and the nondimensionalized heat transfer rate are essentially independent of time. For times from 900 to 1100 s, the temperature at this location decreases significantly with time. However, although the measured temperature decreases with time during this period, the dimensionless heat transfer rate remains nearly constant. The sudden increase both in the temperature and in the dimensionless heat transfer rate at

Table 1 Trajectory points for STS-2 re-entry, as taken from Ref. 9

U_∞, m/s	Altitude, km	M_∞	α, deg	δ_{BF}, deg
6920	72.4	24.30	39.4	14.91
5617	64.4	18.07	41.2	13.54
4168	54.8	12.86	39.7	12.92

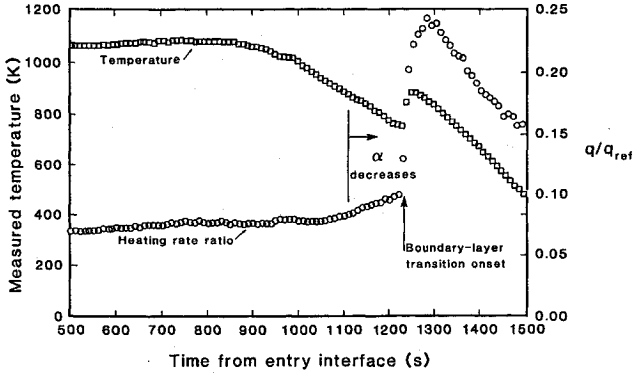

Fig. 2 Temperature and heating-rate histories for V07T9468A (X = 0.297L) for STS-54.

1200 s occurs because the onset of boundary-layer transition passes this point.

Computed Heat Transfer Rates

It is always desirable to compare experimental values with comparable computed values, and vice versa. Flowfield computations,[9] which had been generated for three trajectory points during the re-entry of STS-2, were made available to the present authors. The freestream conditions for these three points are presented in Table 1. A multiblock, laminar heating analysis was performed using the LAURA to generate the heating rates presented in Ref. 9. A seven-species, chemical-nonequilibrium model was used to compute the heating rates presented in this paper for all three flow conditions of Table 1. A finite-catalytic-wall model appropriate for Shuttle tiles at a radiative-equilibrium wall temperature was applied. The local heat transfer rates, which were computed using a value $\varepsilon = 0.9$ (Ref. 9), were nondimensionalized by dividing them by the stagnation-point heat transfer rate given by Eq. (3).

Comparisons of Heat Transfer Rates

For the present paper, time was chosen as the specific parameter at which experimentally determined heat-transfer-rate distributions from the different flights would be compared. Three times were chosen with the requirement that the stagnation-point heat transfer rate for these times most nearly matches that for each of the three flight conditions of Table 1. Thus, data are presented for times of 550 s (which corresponds to Mach 24.30 of Table 1), 900 s (Mach 18.07), and 1050 s (Mach 12.86).

Comparing the experimental values of the heat transfer at a particular time during re-entry, as determined using the temperature measurements in Eqs. (1–3), with existing values computed for the STS-2 flight[9] introduces additional considerations. Although the re-entry trajectories are roughly similar for all missions, there are flight-to-flight variations in various parameters that could have a measurable effect on the heat transfer. Thus, whenever one selects a particular variable (e.g., time) to specify the conditions at which comparisons of the heat transfer distributions will be made, the researcher should recognize that other important parameters may differ from flight to flight. For instance, if one chooses to compare the computed heat-transfer-rate distributions[9] with the experimentally determined distributions for STS-54 at a Mach number of 24.3, other parameters for the STS-54 re-entry will be $U_\infty = 7064$ m/s, altitude = 72.4 km, and $\alpha = 39.86$ deg. Thus, the other parameters will also be fairly close to those presented in Table 1. However, for a Mach number of 18.1, other parameters for the STS-54 flight will be $U_\infty = 5655$ m/s, altitude = 64.3 km, and $\alpha = 39.68$ deg. Approximate heating calculations were made to estimate the effect of changing the angle of attack from 41.2 deg (the Table 1 value) to 39.7 deg. This difference in the angle of attack produced a change of approximately 7% in the heating rates.

Heat-Transfer-Rate Distributions

Nondimensionalized heat transfer rates from recent flights of the Columbia (OV-102) and of the Endeavour (OV-105) are presented in Figs. 3 (distributions along the plane of symmetry) and 4 (transverse distributions). These two vehicles were chosen, because they have the greatest number of thermocouples in the present MADS instrumentation package; see Fig. 1. The data designated OV-102 data in Figs. 3, 4, 8, and 9 are taken from flights STS-28, STS-32, STS-35, STS-40, STS-50, STS-52, STS-55, and STS-58. Those designated OV-105 data are taken from flights STS-47, STS-49, STS-53, and STS-57. Included for comparison are the experimentally determined heat-transfer-rate distributions for the STS-2 [which were recomputed using the emissivity of Eq. (2)]. As noted earlier, the data for the STS-2 mission will be treated as a special case even though the Orbiter flown for the STS-2 mission was Columbia (OV-102), since its aerothermodynamic instrumentation package was the more complete DFI package. Also included for comparison are the LAURA-computed heat transfer rates for Mach 24.30, 18.07, and 12.86. The reader should refer to Ref. 9 for comparisons of the LAURA computations with Orbiter re-entry data, based on a common set of assumptions.

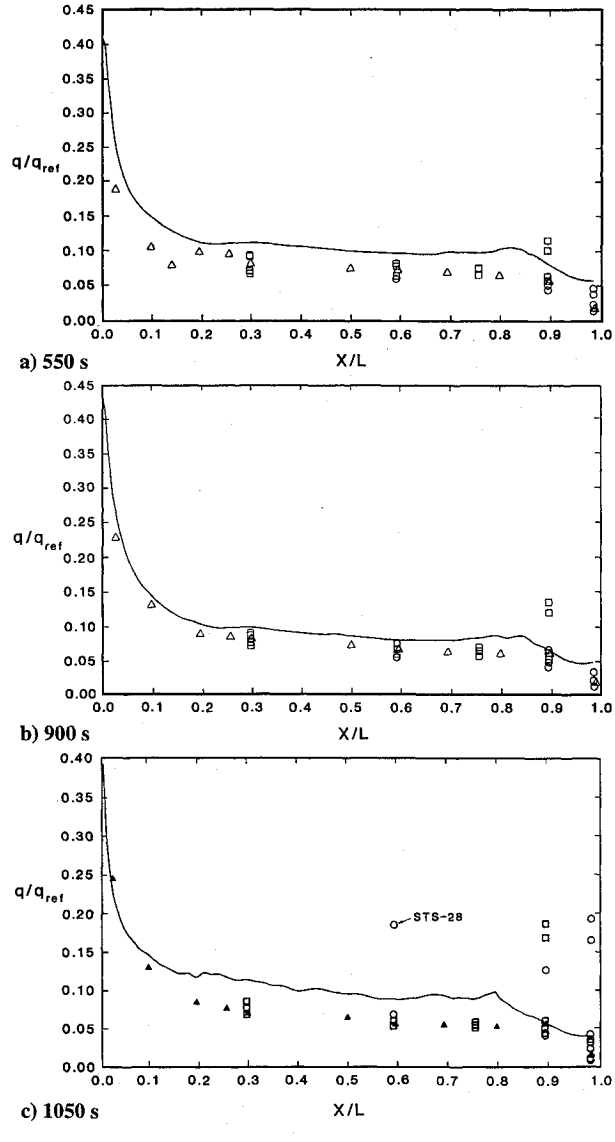

Fig. 3 Heating-rate distributions along the windward plane of symmetry: ——, LAURA; ○, OV-102 data; □, OV-105 data; △, STS-2 data; and ▲, STS-2 data.

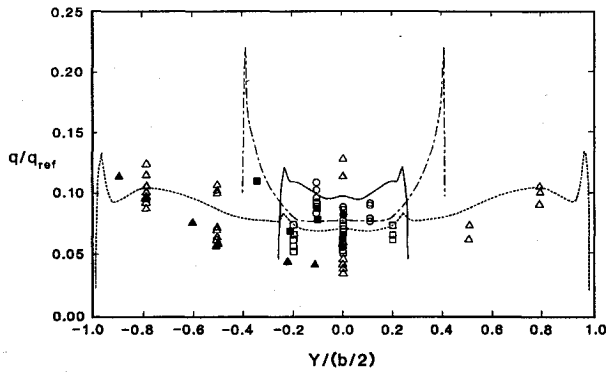

Fig. 4 Transverse heating-rate distributions for the Orbiter at 900 s: ——, $X/L = 0.30$—LAURA; - - -, $X/L = 0.60$—LAURA; - - - -, $X/L = 0.87$—LAURA; ○, $X/L = 0.30$—flight data; □, $X/L = 0.59$—flight data; △, $X/L = 0.87$—flight data; ●, $X/L = 0.30$—STS-2; ■, $X/L = 0.60$—STS-2; and ▲, $X/L = 0.87$—STS-2.

The experimentally determined heat transfer rates for thermocouples located in the plane of symmetry are presented in Fig. 3 for re-entry times of 550, 900, and 1050 s. With a few exceptions, these rates exhibit little scatter. For several flights of the OV-102, the temperature histories for the thermocouples at $X = 0.894L$ and at $X = 0.987L$ indicate that transition has already occurred at these locations by 1050 s. In fact, as indicated in the heat transfer distribution presented in Fig. 3c, the transition front has moved upstream of the thermocouple at $X = 0.592L$ by 1050 s for STS-28. The nondimensionalized heat-transfer rates determined from the temperature measurements of the thermocouple at $X = 0.894L$ are relatively high for all three times for flights STS-47 and STS-49 of the Endeavour (OV-105). The present authors have made approximate calculations, assuming the local flow to be fully turbulent. The local heat transfer rates, thus calculated, are in reasonable agreement with the experimental values. However, the existence of a roughness element (or elements) of sufficient size to trip the flow as early as 550 s (when the freestream Reynolds number based on vehicle length would be less than 10^6) on two different flights is very hard to believe. Unfortunately, this is the downstream-most thermocouple on OV-105, so there are no data farther downstream to provide additional information regarding the character of the boundary layer. The possibility that the high heat transfer rates were due to viscous–inviscid interactions created by the deflected body flap was considered. However, as will be discussed subsequently, with the exception of the measurements for these two flights, the experimentally determined heat transfer rate for this thermocouple was equal to the undisturbed value when the upstream boundary layer is laminar. Thus, there is no clear fluid-dynamics-based phenomenon that would explain these relatively high heating rates. Perhaps there was an instrumentation problem.

Transverse distributions of the heat transfer rates at 900 s for recent flights of the OV-102 and of the OV-105 are presented in Fig. 4 for three X stations, viz., $X \approx 0.3L$, $\approx 0.59L$, and $\approx 0.87L$. These are the three X stations where there are at least three thermocouples in a transverse plane for the post-DFI flights. At first glance, there appears to be considerable scatter in the data. However, careful examination indicates that this is not the case. Consider the heat transfer rates from the plane of symmetry, i.e., $Y/(b/2) = 0$. With the exception of two measurements that exceed $0.11q_{\text{ref}}$, the measured values of the heating rate vary from $0.03q_{\text{ref}}$ to $0.09q_{\text{ref}}$. Referring to the data for these three stations, as presented in Fig. 3b, it can be seen that most of the apparent scatter of the data presented in Fig. 4 reflects the fact that the heat transfer decreases with increasing X. The two measured heat transfer rates from the plane of symmetry that exceed $0.11q_{\text{ref}}$ are from STS-47 and STS-49. As discussed earlier, the reason why these two measurements are consistently high is not known.

Furthermore, the experimental laminar heating rates presented in Fig. 4 exhibit the same dependence on the Y coordinate as do the computed heating rates (taken from the existing solutions[9]). Thus, the simple data-reduction procedure utilizing Eqs. (1–3) provides reasonable experimentally determined heat-transfer-rate distributions (both longitudinal from the plane of symmetry and transverse from a plane on the wing). Measurements that departed significantly from the correlation between experiment and computation were from flights for which the data need further investigation or for which early transition occurred.

Viscous–Inviscid Interactions Due to Body-Flap Deflections

The positive deflection of the Orbiter body flap creates a shock wave, which interacts with the boundary layer on the Orbiter. The adverse pressure gradient produced by the shock wave causes the approach boundary layer to thicken and, for many conditions, to separate, as shown in the sketch of Fig. 5. The extent of the upstream influence of the shock-wave–boundary-layer interaction depends on the size of the subsonic portion of the approach boundary layer and on the strength of the shock wave produced by the turning of the flow. Thus, as noted in Ref. 15, the parameters that influence the extent of an interaction are 1) whether the approach boundary layer is laminar or turbulent, 2) the Mach number of the approach flow, 3) the Reynolds number of the approach flow, 4) the surface temperature, 5) the deflection angle of the ramp, and 6) the chemical state of the gas. Data from the post-DFI Shuttle flights will be examined in this section to see if the simple data-reduction procedure utilizing Eqs. (1–3) applied to the sparse instrumentation can be used to provide insights into the viscous–inviscid interactions due to body-flap deflections.

The current Columbia (OV-102) has four thermocouples in the vicinity of the body flap. Since none of the other three currently operational Orbiters has more than one thermocouple in the body-flap region, the discussion of post-DFI data considers only the OV-102 flights. The OV-102 has three thermocouples in the plane of symmetry ($Y = 0$): one at $X = 0.894L$ (V07T9498A), another at $X = 0.987L$ (V07T9492A), and the third at $X = 1.024L$ (V07T9502A). The locations of these three thermocouples are shown in Fig. 5. The fourth thermocouple in the body-flap region is at the aftmost station ($X = 1.024L$), off the plane of symmetry near the edge of the body flap ($2Y = 0.237b$). Refer to Fig. 1 for the location of all four thermocouples. By correlating the body-flap deflection histories with the experimentally determined heat transfer rates from the Columbia's thermocouples, one can obtain information about the viscous–inviscid interactions due to the body-flap deflections. Data from the flights of STS-28 and of STS-50 will be examined in this section. These two flights of OV-102 were chosen because their body-flap deflection histories were so different that they produced significantly different viscous–inviscid interactions. The histories are presented in Fig. 6. Note that the body-flap deflection angles for STS-28 are more than twice those for STS-50.

STS-28

For times less than 840 s of the STS-28 flight, the body flap is deflected 12.5 deg. As can be seen in Fig. 7a, the heating rate at the upstream-most thermocouple (V07T9489A, $X = 0.894L$) is constant during this time interval and is approximately $0.04q_{\text{ref}}$. The experimental heating-rate distributions for the plane of symmetry in this region are presented in Fig. 8 for the various flights of OV-102. Since the measurements from the thermocouple at $X = 0.894L$ are in reasonable agreement with the computed values, it is believed that the approach boundary layer is attached and laminar. The heating rate at the thermocouple nearest the hinge line (V07T9492A,

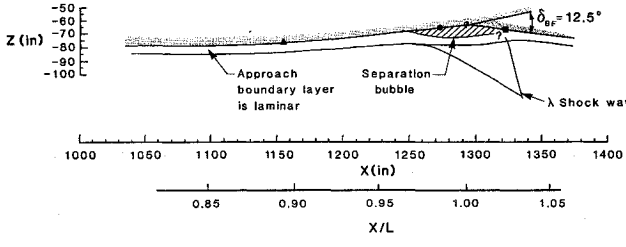

Fig. 5 Sketch of the proposed viscous–inviscid interaction flow model for STS-28 at t = 500 to 800 s, δ_{BF} = 12.5 deg: ▲, V07T9489A; ●, V07T9492A; and ■, V07T9502A.

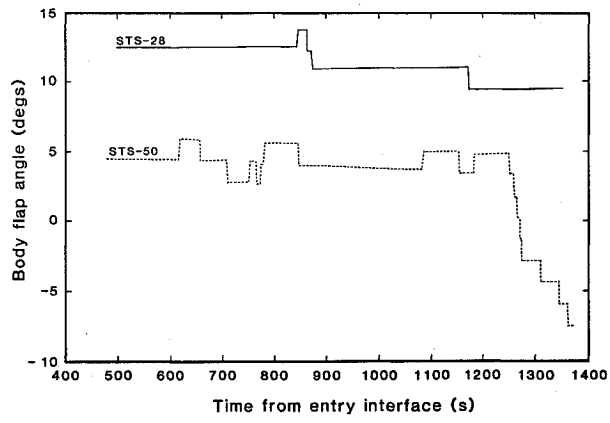

Fig. 6 Orbiter body-flap deflection histories for STS-28 and for STS-50.

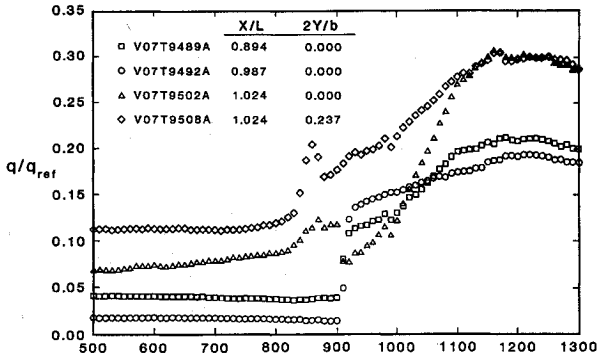

a) STS-28

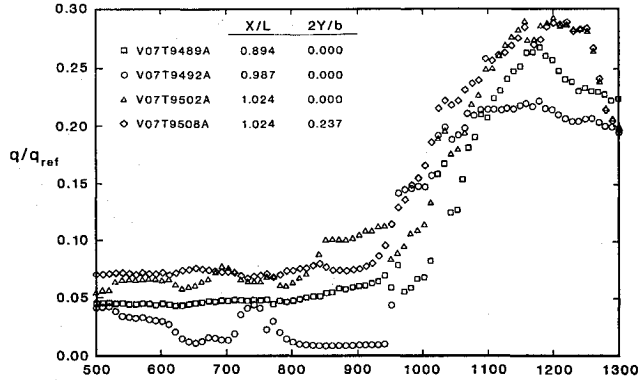

b) STS-50

Fig. 7 Experimentally determined heating-rate histories in the body-flap region.

$X = 0.987L$) is also constant, but relatively low, indicating that this thermocouple is in a region of separated flow. This is consistent with the computed heat-transfer-rate distribution presented in Fig. 8, which indicates a separation bubble in the vicinity of $X = L$. For times of 840 s or less, the heating rates for the two thermocouples at $X = 1.024L$ are significantly higher than the attached, laminar value upstream of the separation bubble (i.e., at $X = 0.895L$). Refer to Fig. 7a. At $X = 1.024L$, the heating rate near the edge of the flap (V07T9508A, $2Y = 0.237b$) is much higher than that in the plane of symmetry (V07T9502A, $Y = 0$). These last two facts suggest a three-dimensional flow with reattachment occurring somewhere in the vicinity of these two downstream-most thermocouples. The sketch of the flowfield model for the plane of symmetry, presented in Fig. 5, is consistent with these observations. A question mark appears in the sketch to reflect the uncertainty as to where the flow reattaches (and/or separates, for that matter).

At 840 s, the body-flap deflection is increased to approximately 14.0 deg and then decreased to 11.0 deg, where it remains for

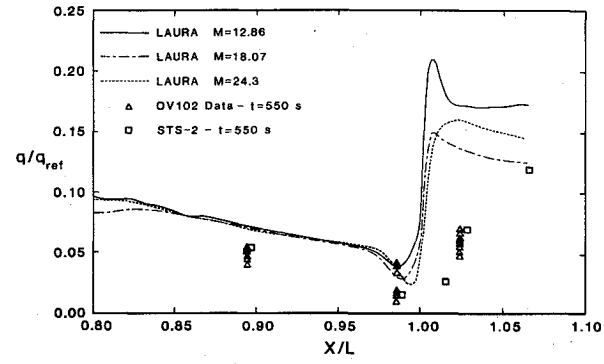

Fig. 8 Heating-rate distributions in the body-flap region.

times from 860 to 1060 s. The body-flap pulse generates a significant increase in heating sensed by the two thermocouples at $X = 1.024L$, as is evident in the measurements presented in Fig. 7a. Again, the thermocouple near the edge of the body flap experiences the greater increase in heating, indicating that the interaction is three-dimensional. The authors believe that the higher heating at the thermocouple at $2Y = 0.237b$ indicates that reattachment occurs at a smaller X/L value near the edge of the body flap than near the plane of symmetry. The heating rates sensed by the two upstream-most thermocouples are essentially unchanged by the body-flap pulse. Thus, the approach boundary layer and the upstream end of the separation bubble are not significantly affected by the slight increase and subsequent decrease in body-flap deflection angle.

Just after $t = 900$ s, the heating rates determined from temperature histories of thermocouples V07T9489A, $X = 0.894L$, and V07T9492A, $X = 0.987L$, increase abruptly with time. See Fig. 7a. Coupled with the heat-transfer distribution presented in Fig. 3a, it appears that boundary-layer transition has moved forward of the two upstream-most thermocouples. The concurrent increase in the heating rate at the thermocouple just upstream of the hinge line (V07T9492A, $X = 0.987L$) indicates that it is no longer in a separation bubble at this time, but is subjected to an attached, transitional boundary layer.

STS-50

Although the body flap undergoes many cycles during the STS-50 flight, the deflection angle remains between 3 and 6 deg, as shown in Fig. 6. With the body flap deflected approximately 4.5 deg at 500 s, the fact that the heat transfer rate at $X = 0.987L$ (V07T9492A) is only slightly less than that at $X = 0.894L$ (V07T9489A), as can be seen in Fig. 7b, indicates that the boundary layer is laminar and attached at both locations. However, at approximately 530 s, the temperature sensed by thermocouple V07T9492A ($X = 0.987L$) decreases measurably, while that sensed by thermocouple V07T9502A ($X = 1.024L$) increases measurably. These changes in the temperature histories are reflected in the experimentally determined heat transfer rates presented in Fig. 7b. There is no significant change in the temperatures recorded at this time by the other two thermocouples located in this region, i.e., V07T9489A ($X = 0.894L$) and V07T9508A ($X = 1.024L$, $2Y = 0.237b$). This is also reflected in the heating rates presented in Fig. 7b.

At 620 s of the STS-50 re-entry, when the body-flap deflection angle is increased from 4.5 to 6.0 deg, there is a sudden decrease both in the temperature sensed by V07T9492A (the thermocouple at $X = 0.987L$, just upstream of the hinge line) and in that sensed by V07T9502A (the thermocouple at $X = 1.024L$, downstream of the hinge line). These temperature histories indicate that the upstream thermocouple is in a separation bubble and the downstream thermocouple is near (perhaps slightly upstream of) the reattachment. Therefore, the flow should be similar to that depicted in the sketch of Fig. 5, even for this relatively small body-flap deflection.

Although it is not as clearly evident in the heat-transfer-rate histories for V07T9492A ($X = 0.987L$) presented in Fig. 7b, the histories of the temperature sensed by this thermocouple (which are not presented in this paper but were used to calculate the experimentally

determined heat transfer rates presented in Fig. 7b) clearly track the body-flap motion. Each time there was a change in the body-flap deflection angle (refer to Fig. 6), there was a change in the slope of the temperature history recorded by this gauge. However, because of the differing time scales for body-flap motion and for wall-temperature response, one should not expect the convective heating rate to follow closely the reradiative heating rate for these regularly changing flowfields. Nevertheless, it appears that, by the holding the body-flap deflection constant at 3.0 deg for times from 705 to 750 s, the temperature sensed by the thermocouple just upstream of the hinge line (i.e., V07T9492A at $X = 0.987L$) has had time to adjust. Thus, the fact that the heating rate at V07T9492A at 750 s is only slightly less than that at V07T9489A ($X = 0.894L$) indicates that there is no separation bubble for this low body-flap deflection angle, i.e., 3.0 deg.

Concluding Remarks

The temperature histories from selected thermocouples for flights STS-26 through STS-58 of the Space Shuttle Orbiter have been analyzed. Equations (1–3) were used to determine nondimensionalized heat transfer rates from these temperature measurements. A primary objective of the analysis conducted for the present paper is to evaluate the heat transfer rates calculated using this simple, state-of-the-art engineering procedure. The rates so determined have been compared with existing computed values and with data from the re-entry of STS-2. They have also been used to relate the motion of the body flap to the viscous–inviscid interactions produced by that motion.

It is believed that the nondimensionalized heat transfer rates provided by Eqs. (1–3), if consistently applied, are of suitable accuracy for the purposes of the present paper. Thus, this procedure can be used to examine (in a timely fashion) all of the temperature measurements from each of the Shuttle Orbiter flights for indications of anomalies in the re-entry environment, as described briefly in the Introduction. Examples of such anomalous behavior include early and/or asymmetric boundary-layer transition and viscous–inviscid interactions, such as the effects of body-flap deflections on the local heat transfer.

Acknowledgments

The authors would like to thank Peter Gnoffo of NASA Langley Research Center for providing the Orbiter flowfield solutions computed using the LAURA code. The authors would also like to thank Timothy Valdez for helping prepare figures for this paper.

References

[1]Bornemann, W. E., and Surber, T. E., "Aerodynamic Design of the Space Shuttle Orbiter," *High Angle of Attack Aerodynamics*, AGARD CP-247, Paper 11; Fluid Dynamics Panel Symposium, Sandefjord, Norway, 1978.

[2]Throckmorton, D. A., "Shuttle Entry Aerothermodynamic Flight Research: The Orbiter Experiments Program," *Journal of Spacecraft and Rockets*, Vol. 30, No. 4, 1993, pp. 449–465.

[3]Goodrich, W. D., Derry, S. M., and Bertin, J. J., "Shuttle Orbiter Boundary Layer Transition at Flight and Wind Tunnel Conditions," *Shuttle Performance: Lessons Learned*, NASA CP-2283, 1983, pp. 753–779.

[4]Stewart, D. A., Rakich, J. V., and Lanfranco, M. J., "Catalytic Surface Effects on Space Shuttle Thermal Protection System During Earth Entry of Flights STS-2 Through STS-5," *Shuttle Performance: Lessons Learned*, NASA CP-2283, 1983, pp. 827–845.

[5]Scott, C. D., "A Review of Nonequilibrium Effects and Surface Catalysis on Shuttle Heating," *Shuttle Performance: Lessons Learned*, NASA CP-2283, 1983, pp. 865–889.

[6]Rakich, J. V., Stewart, D. A., and Lanfranco, M. J., "Catalytic Efficiency of the Space Shuttle Heat Shield," *Entry Vehicle Heating and Thermal Protection Systems: Space Shuttle, Solar Starprobe, Jupiter Galileo Probe*, edited by P. E. Bauer and H. E. Collicott, Vol. 85, Progress in Aeronautics and Astronautics, AIAA, New York, 1982, pp. 97–122.

[7]Anon., *Shuttle Performance: Lessons Learned*, NASA CP-2283, 1983.

[8]Anon., *Orbiter Experiments (OEX) Aerothermodynamics Symposium*, NASA CP-3248, 1995.

[9]Gnoffo, P., Weilmuenster, K., and Alter, S., "A Multiblock Analysis for Shuttle Orbiter Re-Entry Heating from Mach 24 to Mach 12," *Journal of Spacecraft and Rockets*, Vol. 31, No. 4, 1994, pp. 367–377.

[10]Williams, S. D., and Curry, D. M., "An Analytical and Experimental Study for Surface Heat Flux Determination," *Journal of Spacecraft and Rockets*, Vol. 14, No. 10, 1977, pp. 632–637.

[11]Bouslog, S. A., and Cunnington, G. R., "Emittance Measurements of RCG Coated Shuttle Tiles," AIAA Paper 92-0851, Jan. 1992.

[12]Edwards, S. F., Kantsios, A. G., Voros, J. P., and Stewart, W. F., "Apparatus Description and Data Analysis of a Radiometric Technique for Measurements of Spectral and Total Normal Emittance," NASA TN D-7798, Feb. 1975.

[13]Throckmorton, D. A., "Benchmark Determination of Shuttle Orbiter Entry Aerodynamic Heat Transfer Data," *Journal of Spacecraft and Rockets*, Vol. 20, No. 3, 1983, pp. 219–224.

[14]Detra, R. W., Kemp, N. H., and Riddell, F. R., "Addendum to Heat Transfer to Satellite Vehicles Reentering the Atmosphere," *Jet Propulsion*, Vol. 27, No. 12, 1957, pp. 1256, 1257.

[15]Bertin, J. J., *Hypersonic Aerothermodynamics*, AIAA Education Series, AIAA, Washington, DC, 1994.

J. C. Adams
Associate Editor